ISSN 0965-545X, Polymer Science, Ser. A, 2015, Vol. 57, No. 5, pp. 656–666. © Pleiades Publishing, Ltd., 2015.

Permeability of Hydrated Poly(vinyl alcohol): Effect of Relaxation Behaviors and Hydrogen Bonds in Supramolecular Structure[1]

L. Huang and J. H. Wang

Research Center of Advanced Functional Materials and Optical Engineering, Department of Physics, Yantai University, Yantai 264005, China

e-mail: pupolymer@163.com

Received October 15, 2014;
Revised Manuscript Received March 24, 2015

Abstract—The particular permeability of hydrated poly(vinyl alcohol) (PVA) was investigated from the point of polymeric relaxation behavior, and the more essential effect of hydrogen bonds in supramolecular structure was further analyzed as well. The permeability measurement showed that various hydrated PVA samples all had lower permeability to non-polar solvents, and the permeability was affected by relaxation state, which can be controlled by water content. Dynamic mechanical analysis measurements indicated that, in PVA with lower water content the relaxation motion benefiting permeation almost became frozen in glassy amorphous region, due to high activation energy of conformation transition, which then induced the slower permeation to occur. Solid-state ^{1}H and ^{13}C NMR spectra of hydrated PVA samples allowed to analyze the effect of hydrogen bonds. It was found that in PVA with lower water content conformation transition in amorphous region was restricted by more intermolecular and intramolecular hydrogen bonds, especially by the former. Also relatively added crystalline regions, which can affect permeability as physical cross-linking points, were mainly constructed by chain segments with no intramolecular hydrogen bonds. Above results suggest that intermolecular and intramolecular hydrogen bonds via conformation transition control relaxation behavior. Consequently, the relaxation behavior affects the permeability of hydrated PVA, in which water play an important role.

DOI: 10.1134/S0965545X15050107

INTRODUCTION

As is well-known, polymers are permeable, and permeability is an important characteristic of polymeric materials. Many significant applications of polymeric materials depend upon the permeability, such as barrier, separation, controlled release, dyeing, and so on. For containing and packing materials, low permeability means good barrier property, but this property of many polymers is less effective than desired, especially for non-polar solvents. Poly(vinyl alcohol) (PVA) is one of few commercial semi-crystalline polymers with low permeability and excellent barrier property to non-polar solvents. Permeability of some PVA materials have been studied for their actual or potential values in application, such as films or blend films for obstructing gases diffusion [1–3], organic-inorganic hybrid membranes for separating organic mixture [4], cross-linking PVA gel membranes for separating biological solutes [5], and PE/PVA modified blends films against gasoline fuels [6, 7]. Most of these studies were based on the free volume theory and paid more attention to diffusion coefficients and permeation rates.

The fundamental reason for the permeability of polymers is their relatively high levels of creep in comparison with ceramics, glasses and metals [8], so permeation may even be regarded as the results of the relaxation motion of polymer chains. PVA, as most of other polymers, likely has different permeability when its segments have different ability to change conformation, especially in rubbery state and glassy state, respectively. Generally, the thermal relaxation behavior of polymer chains depends upon the segmental rotations, which, for PVA, are closely connected with internal hydrogen bonds. PVA has many multihydroxyl lateral groups, which can further construct supramolecular structure by intramolecular and intermolecular hydrogen bonds. Thus, differing from most other polymers, the relaxation behavior of PVA has close relation with its particular supramolecular structure. Intramolecular and intermolecular hydrogen bonds in supramolecular structure of PVA have attracted much attention of researchers, since PVA is a hydrophilic polymer with the simplest structure [9]. Hydrogen bonds in PVA can be characterized by high-resolution solid-state NMR: ^{1}H NMR spectra can show protons in OH groups with various types of hydrogen bonds and ^{13}C NMR can reveal different OH groups by its directly joined methine, CH. Some

[1] The article is published in the original.

research fields of PVA hydrogel, such as water absorption [10], stereoregularities [11], gelation process [12, 13], structures [14, 15], chain organization and rheological properties [16], has been studied by means of solid-state NMR. The group of Horii has fruitfully studied the relationship among the structures, chain conformation (in crystalline and non-crystalline regions), hydration process and hydrogen bonds of casting PVA films by solid-state ^{1}H and ^{13}C NMR [17–23].

Many researches mentioned in their studies that the permeability of PVA was related to the intermolecular and intramolecular hydrogen bonds in supramolecular structure, but how the hydrogen bonds affect PVA permeability has not been investigated in details. In addition, hydrogen bonds of PVA were studied by solid-state NMR by many researchers, whose research contents did not involve the macroscopic permeability of PVA. Generally, in previous studies, the relaxation states of PVA samples were all controlled by testing temperature [17, 19, 21]. Whereas, as a water-soluble polymer, the relaxation state of PVA also can be controlled by the degree of hydration (the degree of swelling with water). And this characteristic will make it possible that the permeability of various relaxation states samples can be tested at room temperature, avoiding the effect of higher temperatures on the activity of permeants. The corresponding NMR test also can be performed at room temperature, avoiding the effect of higher temperatures on the hydrogen bonds with temperature sensitivity as well. Now, PVA containers obtained by novel thermal processing method can offer feasible testing samples [24], which make it possible that the permeation rate of PVA can be easily obtained by simple weight loss method. In particular, the permeability of a container with single PVA has not been reported for the difficulty of PVA thermal processing, since the melting point of PVA was close to its thermal decomposition temperature.

In this paper, we studied the permeability of PVA in different relaxation states by bottle samples with different degrees of hydration, and the effects of relaxation behavior on them were analyzed by means of DMA as well. To further understand the permeability of PVA, solid-state ^{1}H and ^{13}C NMR were introduced to investigate the intramolecular and intermolecular hydrogen bonds in amorphous region and crystalline region of PVA in different relaxation states, respectively. The main objective of above research is to understand the permeability characteristic of PVA well from the relaxation behavior of polymer chains and the evolution of hydrogen bonds in supramolecular structure.

EXPERIMENTAL

Materials

PVA 1799 (GB12010-89, degree of polymerization 1750, hydrolysis degree 99%) was provided by the Sichuan Vinylon Factory, SINOPEC (China). Samples were washed several times with deionized water until pH 7 was attained, and were dried to constant weight. Deionized water was used throughout the experiments.

Sample Preparation

Deionized water was added into dried PVA powder, and then the mixtures were stored in a sealed container at ambient temperature until the deionized water had permeated well. The prepared mixtures were plasticized and blow-molded into bottles with a capacity of about 500 mL and a wall thickness of 1.0 mm.

Bottles were stored in sealed glass containers with different levels of relative humidity (RH) at 23°C for 28 days to obtain test bottles with various water contents balancing to storage conditions. The exact RH values of storage conditions were controlled by various saturated salt solutions: saturated aqueous solution of LiCl (RH = 11%), $MgCl_2$ (RH = 33%), KBr (RH = 58%), NaCl (RH = 75%) [25, 26]. Besides, storage conditions with RH = 0% is controlled by P_2O_5, and storage conditions with RH = 100% is controlled by pure water. The test bottles were named as B_0, B_{11}, B_{33}, B_{58}, B_{75} and B_{100}, respectively. These salts and P_2O_5 were analytically pure reagents.

Characterization

Permeability of PVA with different water contents was tested by weighting the mass loss of sealed test bottles filled with solvent. These test bottles were stored in previous glass containers with different RH at 23°C for 28 days. During storage, the glass containers were not absolutely sealed and a slit near lid was left to permit slow gas exchange to occur between inner and outside of the containers. The slit can avoid the accumulation of permeated solvents in containers, at same time it will not affect the stationary RH due to a mass of saturated salt solutions at the bottom of the containers. Three parallel sample bottles were taken out for weighing at regular intervals and the permeation rates with test error were obtained. The filled permeants were octane, xylene and methanol, respectively.

The crystallinity and water content of hydrated PVA were tested using DSC (NETZSCH DSC 204). Slices of the above bottles with total weight of 5–7 mg were weighed and sealed in aluminium pans, which had been pretreated in boiling water and dried before use. The pans were heated from ambient temperature to 245°C at a rate of 10 deg/min. The evaporation heat of water and the melting heat of crystalline PVA were obtained by integrating the respective peaks. The

evaporation latent heat of total water, ΔH_w^0 is 2257 J/g [25, 27], the enthalpy obtained by integrating the evaporation peak of total water is ΔH_w, therefore the proportion of water is $\Delta H_w/\Delta H_w^0 \times 100\%$. The latent heat of melting of pure crystalline PVA, ΔH_c^0 is 138.6 J/g [28], the enthalpy obtained by integrating the melting peak of crystalline PVA is ΔH_c and the proportion of PVA in the test sample is R, therefore the crystallinity is $\Delta H_c/(\Delta H_c^0 R) \times 100\%$.

Sheets of size 40 × 5 × 1 mm^3 sheared from PVA bottles with different water contents were measured by DMA (TA Q800). Measurement were in a forced non-resonance tension mode with programming frequencies of 1, 5, 20 Hz, amplitude of 50 μm and force-track of 135.0%. Storage modulus G', loss modulus G'', and loss tangent tanδ, were recorded as a function of temperature over a range of −120 to 100°C (except for B0 with the measure range of −120 to 120°C) with a ramping rate of 2 deg/min. The apparent activation energy of relaxation motion was calculated by an Arrhenius equation. Temperature calibration of DMA was carried out with pure water and pure indium.

Dry PVA powders were annealed at 150°C for 10 min in nitrogen atmosphere, and then were stored in previous glass containers with different RH to obtain various water contents for solid-state NMR measurement. Side-chain deuterated PVA sample (PVA-d_1) was prepared by soaking and sealing PVA powders in 99.9% deuterated water in nitrogen atmosphere for 5 days, and then PVA-d_1 was dried at 50°C for 3 days under vacuum, after which sample was also stored in sealed glass containers with P_2O_5 and annealed as the processes described above.

Solid-state ^{1}H combined rotation and multiple pulse spectroscopy (CRAMPS) NMR and solid-state cross polarization/magic angle spinning (CP/MAS) ^{13}C NMR spectra measurements were performed at room temperature (23°C) on BRUKER AVANCE III 400 spectrometer under static magnetic field of 7.0 T. 4 mm MAS probe was used with the MAS rate of 2.5 KHz for ^{1}H CRAMPS, measurement were performed with the π/2 pulse width and the pulse duration was 1.3 and 3.0 μs, respectively; 4 mm MAS probe was used with the MAS rate of 5.0 KHz for CP/MAS ^{13}C spectroscopy, measurement were performed with the spin-lattice relaxation time (T_{1C}) of 70 s, and spectra were obtained with respect to the methylene carbon resonance of solid adamantine.

Solution-state ^{1}H NMR spectra were also recorded by an BRUKER AVANCE III 400 spectrometer in deuterated dimethyl sulphoxide (DMSO-d_6), revealing that 76.5% OH protons were deuterated for PVA-d_1.

Table 1. Parameters of polymers, permeants and water [29]

	Solubility parameter		Molecule volume[c], nm^3
	δ_P^a, MPa$^{1/2}$	δ_H^b, MPa$^{1/2}$	
PVA	9.0	18.0	–
PET	4.5	12.3	–
PE	2.9	4.1	–
PP	3.0	3.0	–
Octane	0	0	0.27
Xylene	1.0	3.1	0.20
Methanol	12.3	22.3	0.07
Water	16.0	42.3	0.03

[a] Polar cohesion (solubility) parameter. [b] Hydrogen bonding cohesion (solubility) parameter. [c] Calculated by the molar volumes data in [29].

RESULTS AND DISCUSSION

Permeability

Permeation is a combined result of permeant's sorption and diffusion in polymer. The driving force of permeation is provided by the concentration gradient of permeant between inside and outside of PVA bottles. In addition, the concentration gradient depends upon the difference of polarity between permeant and polymer, and it also depends on the interaction among polymer chains. In this study, three organic solvents with different polarity, octane, xylene and methanol were selected as the permeants for permeation tests. The solubility parameters of polymer materials, permeants and water are listed in Table 1, and the permeation rates with the error bars representing three tests of parallel samples are showed in Fig. 1.

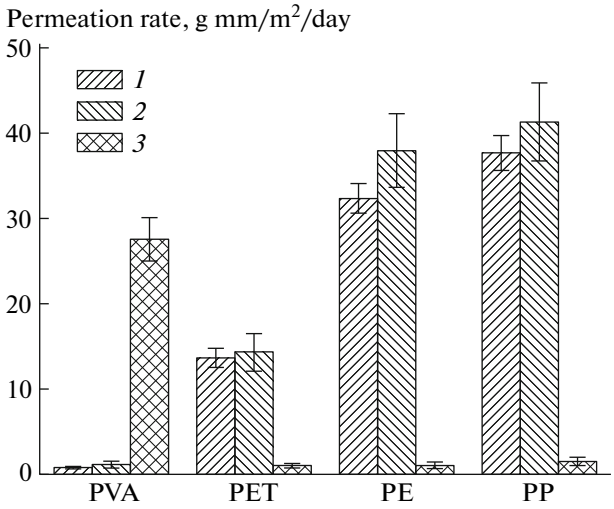

Fig. 1. Permeation rates of different polymer bottles to various solvents: (*1*) octane, (*2*) xylene, and (*3*) methanol.

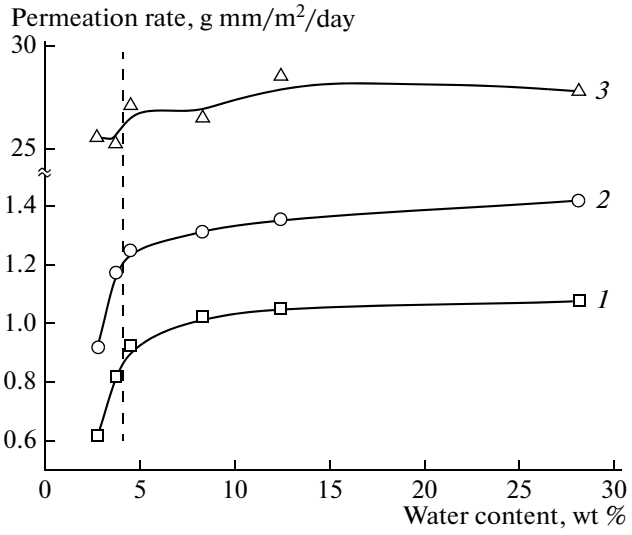

Fig. 2. Permeation rates of PVA bottles with different water contents: (*1*) octane, (*2*) xylene, and (*3*) methanol.

Table 1 and Fig. 1 show the different permeability compared between PVA and PET. The stronger polarity of a polymer means lower permeability to non-polar solvents, when hydrogen bond solubility parameters of them are both high. Comparing the permeability of PET to that of PE and PP also shows that higher hydrogen bond solubility parameters of a polymer means lower permeability to non-polar solvents even though polar parameters are similarly low. In addition, to methanol, a polar solvent, polarity may be the only factor for polymeric permeability. Above results suggest, to non-polar solvents, hydrogen bond in polymer bottle is a key factor for its permeability.

The polarity of a polymer is constant, but the hydrogen bonds between polar groups with hydrogen can be altered by introducing little molecules, especially polar litter molecules. Water, as a high polar little molecule, just can alter hydrogen bonds and then change the permeability of PVA significantly. Permeation rates of PVA bottles with different water contents are shown in Fig. 2. When water content is less than about 4%, the permeation rates of PVA bottles to octane and xylene decrease apparently, though it is not apparent to methanol maybe coming from good solvent effect. To analyze the reason of decreased permeation rate, PVA bottles with different water content are measured by DSC, and the results are listed in Table 2. This table shows that with the decrease of water content, the amorphous phase decrease and crystalline phase increases a few. That means that the amorphous regions at the crystalline/amorphous interface instead fold up into new secondary structures of crystallites with planar zigzag structure. The comparison between B_{100} and B_0 shows that when crystallinity increases from 28.2 to 33.9%, the corresponding permeation rates decreases 42.9 and 35.2% for octane and xylene, respectively. Permeations just occur in the relatively loose amorphous regions, which have no long-range molecular order, and the compact crystalline regions are the impermeable [8, 30]. Whereas, it is obvious that the increased extent of crystalline phase is not sufficient to decrease permeation rate so much.

As is well known, water exists in water-soluble polymeric systems in the form of non-freezable bound water, freezable bound water and free water according to the different hydrogen bonds between water and polymer [31, 32]. Among these forms, only the bound water is the most effective plasticizing water in hydrophilic polymer, because it reduces the inter-chain cohesion by intercepting the intermolecular hydrogen bonds formed by hydroxyl groups [33]. The critical threshold of water content for freezable bound water beginning to appear is about 17.2%, and for free water is about 37.6% [27]. So except for B_{100}, which has a little freezable bound water, there is only non-freezable bound water in bottle samples. The decrease of non-freezable bound water, a high efficient plasticizer, perhaps changes the relaxation state of hydrated PVA and then alters the permeability of it. So it is necessary to study the relationship between relaxation states and permeability of hydrated PVA samples, which has not been reported in details in the references mentioned above.

Relaxation States

Regardless the transition of permeants in diffusive molecular model [34, 35], the redistribution of free volume in diffusive free volume model [36], or the

Table 2. Material parameters of PVA bottles with different degree of hydration

	RH, %					
	0	11	33	58	75	100
Sample	B_0	B_{11}	B_{33}	B_{58}	B_{75}	B_{100}
Water, wt %	2.8	3.7	4.5	8.3	12.4	28.1
Crystallinity, %	33.9	30.4	28.7	28.3	28.4	28.2
Water in amorphous region, wt %	4.2	5.2	6.2	11.2	16.5	35.2
Mean water molecule per structural unit in amorphous region	0.11	0.13	0.16	0.31	0.48	1.33

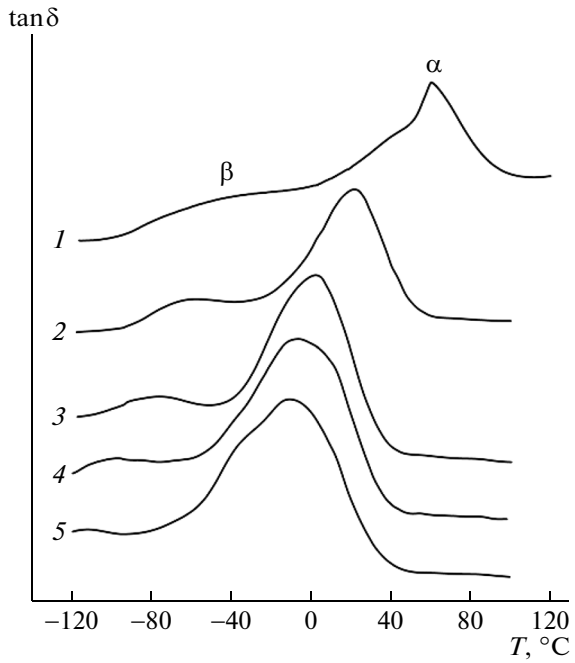

Fig. 3. tanδ spectra of PVA bottles samples (*1*) B_0, (*2*) B_{11}, (*3*) B_{33}, (*4*) B_{58}, and (*5*) B_{75}, with various water contents measured in 1 Hz.

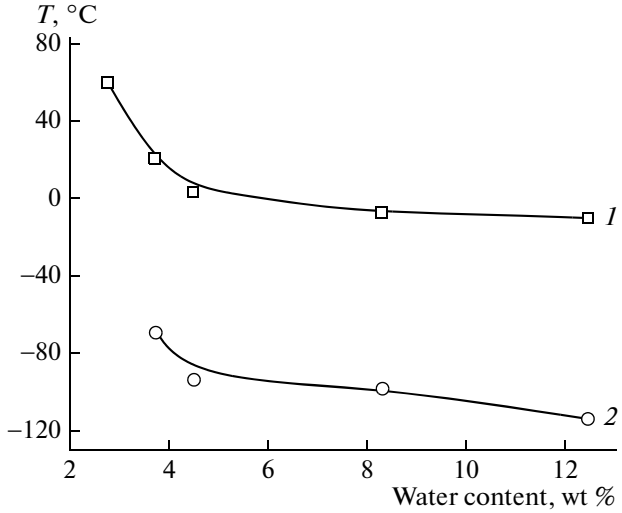

Fig. 4. Relaxation transition peak temperatures (*1*) T_α and (*2*) T_β of PVA bottles samples with various water contents measured in 1 Hz.

close and open of "windows" between adjacent cavities in diffusive molecular dynamic simulation [2, 37, 38], the accomplishment of all these actions involving permeation inevitably strongly depends on the motions of polymer chains, and their mobility is closely connected with the relaxation state of polymer. The different relaxation state, rubbery or glassy state can provide different level of chain segments motion in amorphous regions, where the different permeability of polymer materials for same permeant will be found.

tanδ in dynamic mechanical relaxation spectra of various PVA samples are shown in Fig. 3, and corresponding relaxation transition peak temperatures are shown in Fig. 4. On every tanδ curve, there is a main relaxation peak, α relaxation, corresponding to glass transition of main chain segments, and a secondary relaxation peak, β relaxation, corresponding to slightly cooperative motion of the main chain segments. γ relaxation, another kind of weaker secondary relaxation associated with the motion of side groups, was not found. That is due to mass transfer by rotation of OH around C–OH axis is so small that not any relaxation signature can be detected, and that is in agreement with other researches [39]. It appears that the samples with lower water content have higher α relaxation and β relaxation temperature together with a diminishment of relaxation peak intensity, especially for the former. The temperatures of α and β relaxation peaks are all strongly influenced by the water content, i.e. so-called plasticization effect. The decrease of tanδ intensity and the increase of T_g are ascribed to the result of decreasing irrecoverable viscous flow among the polymer chains, benefiting from physical crosslinking formed by intermolecular interaction.

If a polymer chain changes its conformation, individual C–C bonds must twist from the *trans* to *gauche* position or vice versa, i.e. the torsion angles must change, which is a thermally activated process. Above T_g, the intermolecular interaction is weak and the torsion angles can change with lower energy, so the conformation becomes movable although it also depends on time-scale. From Figs. 2 and 3, we can find that the majority of the permeation takes place once the hydrated PVA enters rubbery state. Here, the relaxation of PVA chains depends on both the main motion of chain segments and the cooperative motion of the chain segments in rubbery amorphous region. These motions can easily induce the redistribution of open spaces, i.e. cavities, where the permeants can be accommodated, and then the permeants will be carried along to move by density fluctuations caused by the thermal motion of surrounding chains. A succession of such small random moves of permeants constitutes the diffusion of permeants. Thus, the formation of a cavity of sufficient size to accommodate a permeant can be viewed as the rate-controlling step for a move [38]. B_{100}, B_{75}, B_{58} and B_{33} are in rubbery state at room temperature, so the rapid permeation occurs with the strong thermal motions of polymer chains. This means PVA chains need shorter time to form cavities with sufficient size to accommodate and transfer these permeants, and the permeability increases with the decrease of interaction among polymer chains for more water molecules. But below T_g, there is not enough thermal energy available to allow torsion angle changes, so the conformation becomes frozen in regardless amorphous region or crystalline region.

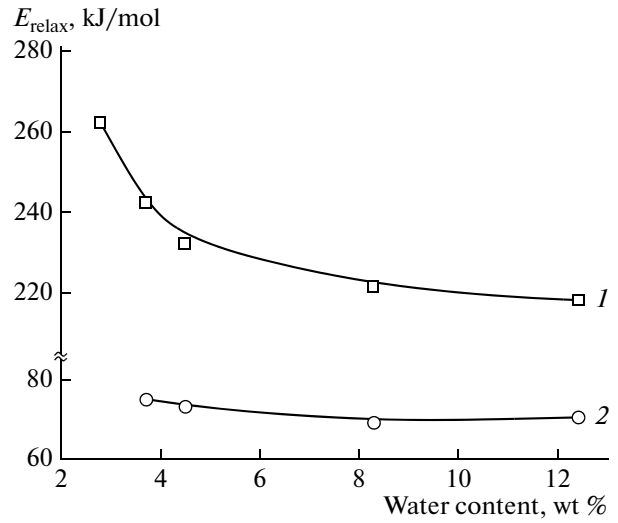

Fig. 5. Apparent activation energy of relaxation motion (*1*) $E_{relax\text{-}\alpha}$ and (*2*) $E_{relax\text{-}\beta}$.

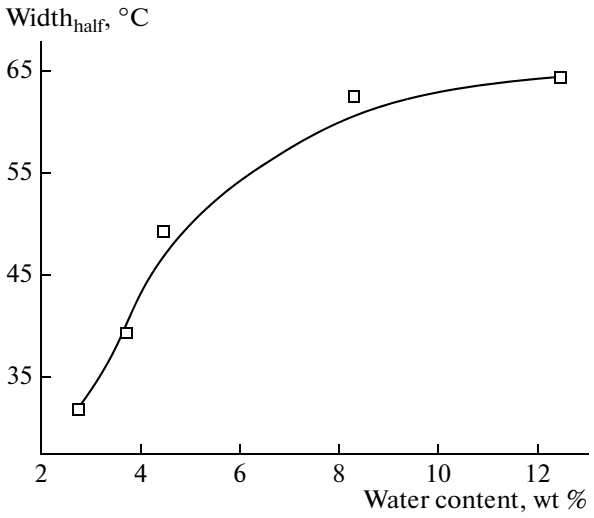

Fig. 6. Width of glassy transition peak at half height.

Then the relaxation behavior of PVA chains only depend on the slightly cooperative motion of the chain segments, the extremely restricted segmental mobility, in glassy amorphous region. At this moment, a permeant spends most of its time in rattling within a cavity and just can occasionally jump from a cavity to the other, thus the overall diffusion process in PVA is obviously slow. B_{11} and B_0 are in glassy state at room temperature, so completely different slow permeation behavior will occur due to different relaxation state of PVA.

To understand the different torsion energy of chain segments above and below T_g, the apparent activation energy of relaxation motion, E_{relax}, was measured by DMA at different frequencies. E_{relax} is proportional to torsion energy, and it can be obtained by the Arrhenius equation

$$f = f_0 e^{-E_{relax}/RT}, \quad (1)$$

where f is frequency, f_0 is pre-exponential factor and R is a constant. The slope of a linear fitting line of $\ln f$ versus $1/T$ presents corresponding E_{relax} of α or β relaxation, $E_{relax\text{-}\alpha}$ or $E_{relax\text{-}\beta}$, which are shown in Fig. 5. And the reciprocal value of its intercept, relaxation time of chain segments, is in the order of 10^{-3} and 10^{-17} s, respectively. $E_{relax\text{-}\alpha}$ of glassy PVA are obviously higher than these of rubbery PVA, which are in corresponding with their mobility. The $E_{relax\text{-}\beta}$ of B_0 is not obtained for the same reason of the overlap of α and β relaxation peaks, so we just can obtain a partial curve of $E_{relax\text{-}\beta}$, which have no significant change trend.

Another important feature of relaxation behavior of hydrated PVA is the tanδ peak width (see Fig. 3). Generally, the breadth of transition region is closely related to the degree of structural heterogeneity, because an inhomogeneous distribution of segmental mobilities leads to a broad distribution of relaxation times [40]. The widths of glassy transition peak at half height (W_{half}) decrease with the increase of T_g (Fig. 6), meaning the distributions of movable chain segment shifts from wider range to narrower range with forming more new points of interaction between polymer chains. The longer segments have high mobility and also have more chance to form new interaction points, thus the homogeneity of chain segments increases by shortening the mean length of longer segments. Such network evolution further causes a homogeneous distribution of segmental mobility, leading to a narrow distribution of relaxation times shown by narrow temperature range of glassy transition. These more interaction points originate from the recovery of intermolecular hydrogen bonds after decreasing water content. In fact, the decrease of tanδ intensity mentioned above also benefits from intermolecular hydrogen bonds, because the change of conformation originated from the rotation of C–C backbone bond angles are largely determined by intermolecular hydrogen bonds in supramolecular structure.

Hydrogen Bonds in Supramolecular Structure

Molecular dynamic simulation has shown that the lifetimes of various hydrogen bonds in PVA are shorter [1]. Thus, we can speculate that old hydrogen bonds associated with PVA hydroxyls are continually untied and new hydrogen bonds are continually tied at the same time. As water is added to polymer chains, it has chance to form new hydrogen bonds with the free hydroxyls coming from the temporary untied hydrogen bonds, which leads to the generally mentioned result that the hydrogen bonds between chains are destroyed and chain are spaced. This result offers space to permeants and also promotes relaxation

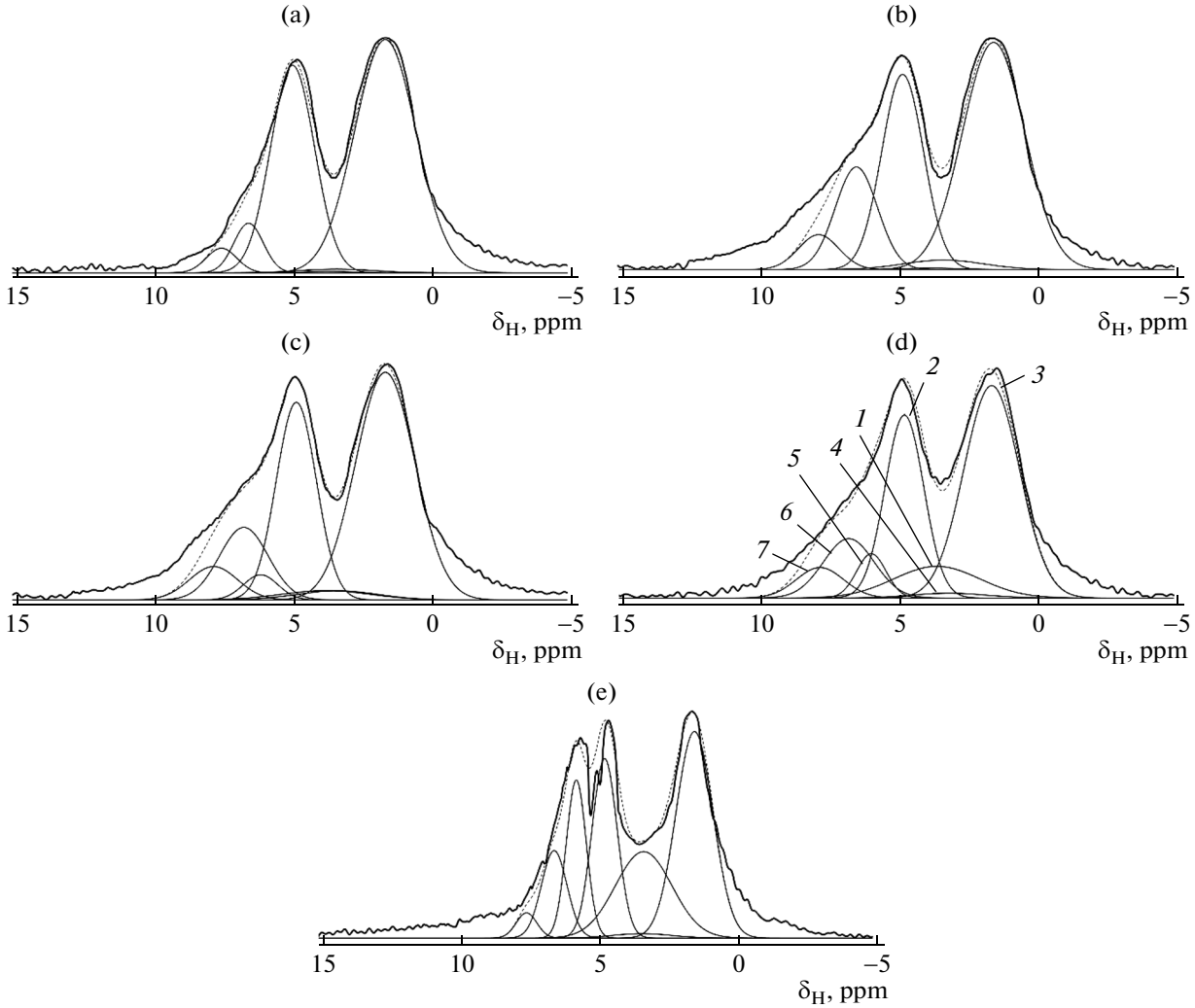

Fig. 7. Solid-state ^{1}H CRAMPS NMR spectra with line shape analysis of (a) a dry PVA sample with partly deuterated side-chain (PVA-d_1) and hydrated PVA samples (b) B_0, (c) B_{33}, (d) B_{75}, (e) B_{100} in different relaxation states (thick solid line: experimental spectra; thin solid lines: respective constituent lines obtained by line shape analysis; broken lines: the linear combination of the respective thin lines). (*1*) Water, (*2*) CH, (*3*) CH_2, (*4*) OH_f, (*5*) OH_r, (*6*) OH_{inter}, and (*7*) OH_{intra}.

motion by conformational changes of PVA chains which allow permeation to occur more readily.

Solid-state ^{1}H NMR spectra can reveal three types of proton in OH groups by line shape analysis developed by Horii et al [19, 21, 22]. These OH groups with different protons include hydrogen-bonded OH_h involving intramolecular OH_{intra} and intermolecular OH_{inter}, OH_f free from hydrogen bond preferentially existing in crystalline region, and highly mobile OH_r in non-crystalline region above T_g. Solid-state ^{1}H CRAMPS NMR spectra of hydrated PVA bottle samples in different relaxation states controlled by water content and a dry PVA sample with partly deuterated side-chain (PVA-d_1) are shown in Fig. 7 with introducing the line shape analysis. In Fig. 7, the thick solid line is experimental spectra, thin solid lines are respective constituent lines obtained by line shape analysis, and broken lines is the linear combination of the respective thin lines. It is found that the chemical shifts of various protons resonance lines keep almost constant with different water content, although their chain conformation is changed evidently in amorphous region above T_g. This result is similar to the result of a PVA sample measured at different temperature [21] and also simplifies the following line shape analysis. A comparison between dry PVA-d_1 (Fig. 7a) and dry sample B_0 (Fig. 7b) indicates the chemical shift position of various OH protons peaks. In Fig. 7e, the peak between CH and OH_{inter} peaks is assigned as OH_r protons [19, 21], and the chemical shift of OH_r protons in other spectra all refer to it. The peaks between CH and OH_{inter} peaks are assigned as H_2O protons [10]. Above assigned resonance lines are all indicated in Fig. 7d. The mole fraction of various pro-

Table 3. Mole fraction of various protons compared to CH_2 proton peaks

	CH_2	CH	$(OH_{intra} + OH_{inter} + OH_f + OH_r)$	H_2O
PVA-d_1	2	1.05	0.24	0.13
B_0	2	1.03	1.07	0.12
B_{33}	2	1.04	1.05	0.21
B_{75}	2	1.05	1.06	0.71
B_{100}	2	1.09	1.17	1.92

tons compared to the integrated areas of corresponding CH_2 proton peaks are shown in Table 3. The ratios of various H obtained by line shape analysis approach the actual ratio (CH_2 : CH : OH = 2 : 1 : 1), the ratios of H involving water approach the water content shown in Table 2, and the ratio of H involving undeuterated side-chain OH is close to the result of solution-state ^{1}H NMR measurement (i.e. deuterated OH protons are about 76.5%). All above results show that the line shape analysis method can provide the approximate composition of various H in hydrated PVA samples. In Fig. 7e, the OH peaks of B_{100} with more water content significantly becomes narrower, which is similar to the effect of increasing temperature [21]. This indicates that the OH groups undergo exchange motion among various hydrogen bond states including OH_f above T_g, and the exchange rate is faster with increasing water content.

The mole fractions of different OH protons obtained by line shape analysis in Fig. 7 are plotted against their water content in Fig. 8, and whole plot is separated into two regions by a dashed line. In region *A*, test temperature (i.e. room temperature) is lower than the T_g of corresponding samples, and samples are in glassy state. In region *B*, test temperature is higher than T_g, and samples are in rubbery state. The mole fractions of OH_{inter}, OH_{intra} and OH_f protons all increase with decreasing water content, but that of OH_{inter} protons show a remarkable increase when they are in glassy state. In contrast, the mole fraction of OH_r protons decreases with decreasing water content and shows a remarkable decrease almost to zero when they are in glassy state. Above results imply OH_{inter} and OH_r protons are more sensitive to the change of water content when they are in glassy state. Highly mobile OH_r are only in non-crystalline region and sample crystallinity has not apparent increase, thus decreased OH_r protons mainly transfer into OH_{inter} and OH_{intra} protons in non-crystalline region. Especially, in region *A*, remarkably decreased OH_r protons mostly transfer into OH_{inter} protons in non-crystalline region, which keep samples in glassy state with stronger intermolecular interaction. The diffusivity is sensitive primarily to the decrease in concentration of intermolecular hydrogen bonds [1], so the above result endow glassy state PVA sample with lower permeability.

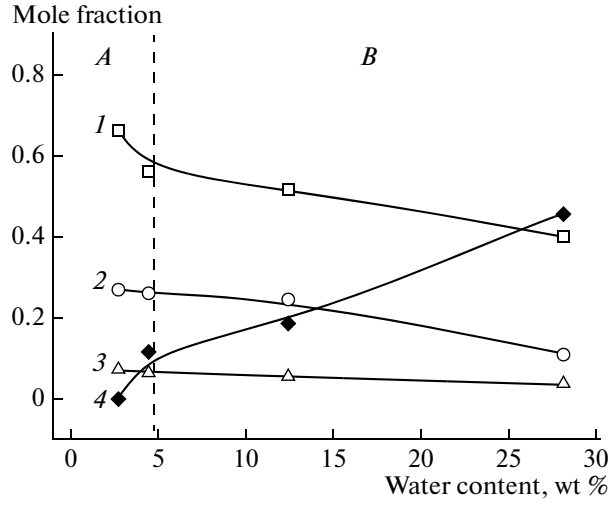

Fig. 8. Mole fractions of different OH protons obtained by line shape analysis against water content. (*1*) OH_{inter}, (*2*) OH_{intra}, (*3*) OH_f, and (*4*) OH_r.

The presence of crystalline domains has another effect on sorption and diffusion behavior of samples, i.e. it acts as a physical cross-linking region to restrict the relaxation motions of amorphous regions, which will then be obstructive to permeation process [8]. Because of the lower molecular mobility of crystalline component, solid-state CP/MAS ^{13}C NMR spectra with longer spin-lattice relaxation time (T_{1C} = 70 s) [20–22] can provide the information of hydrogen bonds in crystalline region. The nature of the ^{13}C spectrum as a function of water content is shown in Fig. 9. There are four peaks remaining almost constant chemical shift for every hydrated sample. The lowest chemical shift peak at 44.9 ppm (peak IV) is attributed to CH_2 carbon, and the triplet peaks at 76.5 ppm (peak I), 70.1 ppm (peak II) and 64.6 ppm (peak III) are associated with CH carbon, which can be approximatively thought are completely linked to OH of PVA with hydrolysis degree 99%. These CH carbon peaks, in the order of decreasing chemical shift, can be assigned to the mm (isotactic) sequences with two intramolecular hydrogen bonds, the mm and mr (heterotactic) sequences with one intramolecular hydrogen bond, the mm, mr and rr (syndiotactic) sequences with no intervening intramolecular hydrogen bonds, respectively [9, 10, 11, 12, 41]. B_0 with low water content in glassy state show a broader peaks including triplet CH_2 carbon and CH carbon (except for peak I), which indicates more dispersive chemical shifts of them. The freezing of free rotation of chain segments leads to forming fixed conformations with different chemical shifts, i.e. the nonequivalence of various conformations coming from different geometrical arrangements of the interacting groups. From the

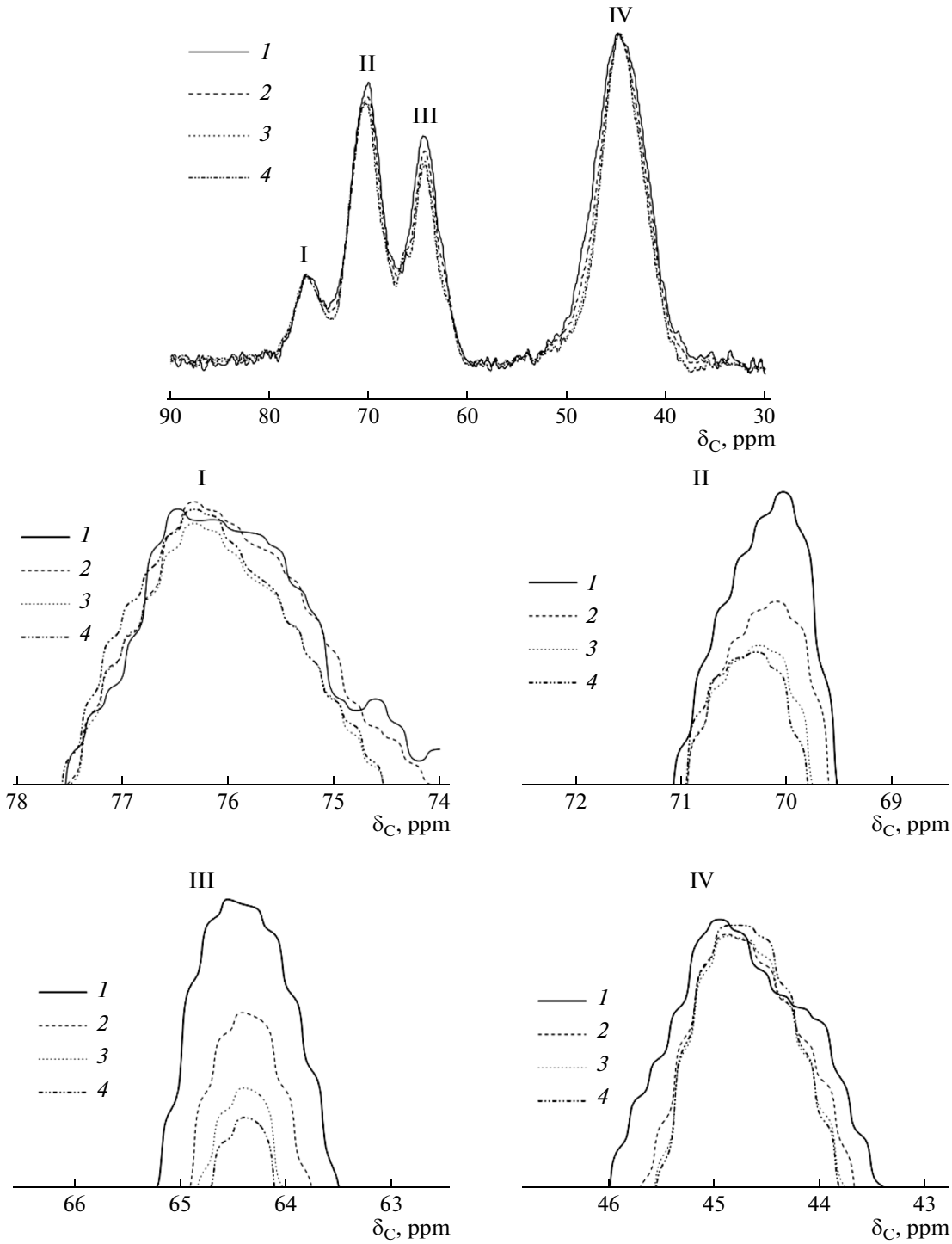

Fig. 9. Solid-state ^{13}C CP/MAS NMR spectra of dry and hydrated PVA samples (*1*) B_0, (*2*) B_{33}, (*3*) B_{75}, and (*4*) B_{100} in different relaxation states.

particular structure of PVA, it can be thought that the peaks broadening is a result of dehydration that increases the ^1H dipole-dipole interactions coming from more intramolecular hydrogen bonds, which then decreases the molecular mobility compared with the hydrated samples. At the same time, even though B_{100}, being in rubbery state with 28.1 wt % water, there also is some hydrogen bonds because it does not show sharp peaks indicating solution-like behavior in solution-state NMR spectra. The width of peak I almost have no obvious change, showing that the conformation mobility of CH carbon with

Table 4. Ratio between integrated areas of each CH peak and that of CH_2 peak

	CH			CH_2 Peak IV
	Peak I	Peak II	Peak III	
B_0	0.12	0.48	0.42	1
B_{33}	0.14	0.47	0.40	1
B_{75}	0.16	0.47	0.38	1
B_{100}	0.16	0.48	0.38	1

two intramolecular hydrogen bonds is not apparently changed with decreasing water content.

To compare the carbon content of each corresponding CH peaks, we assume the integrated area of CH_2 peak is equal to 1, and the ratio between integrated areas of each CH peak are listed in Table 4. The approximate comparison of corresponding CH carbon content indicates that, with the decrease of water content, CH carbon with two intramolecular hydrogen bonds decrease, CH carbon with one intramolecular hydrogen bond almost have no apparent change, and CH carbon with no intramolecular hydrogen bond increase. Above results mean that more crystalline regions are mainly constructed in low water content samples by chain segments with no intramolecular hydrogen bonds. The newly added crystalline regions will also play an important role in restraining the relaxation motions of amorphous regions, and then affect permeation process.

CONCLUSIONS

The particular permeability of hydrated PVA was investigated from its relaxation behavior and hydrogen bonds in supramolecular structure, and following conclusions were obtained.

Differing from other polymeric materials, various hydrated PVA samples all had lower permeability to non-polar solvents, and the permeability was affected by the relaxation state which can be controlled by water content.

In the PVA with low water content, the relaxation motion benefiting permeation almost became frozen in glassy amorphous region due to high activation energy of conformation transition, which then induced the slowest permeation to occur.

In the PVA with low water content, conformation transition in amorphous region was restricted by more intermolecular and intramolecular hydrogen bonds, especially by the former.

Newly added crystalline region which can affect permeability as physical cross-linking points were mainly constructed by chain segments with no intramolecular hydrogen bonds. Crystalline region played an important role in restraining chains motion and restrict its relaxation behavior, and it can affect permeability as physical cross-linking points more than as physical barrier region.

In short, intermolecular and intramolecular hydrogen bonds via conformation transition control relaxation behavior, and then finally affect on the permeability of hydrated PVA, where water play an important role.

REFERENCES

1. G. E. Karlsson, U. W. Gedde, and M. S. Hedenqvist, Polymer **45**, 3893 (2004).
2. I. Cozmuta, M. Blanco, and W. A. Goddard, J. Phys. Chem. B **111**, 3151 (2007).
3. J. Jang and D. K. Lee, Polymer **45**, 1599 (2003).
4. F. Peng, L. Lu, H. Sun, Y. Wang, H. Wu, and Z. Jiang, J. Membrane Sci. **275**, 97 (2006).
5. H. Matsuyama, M. Teramoto, and H. Urano, J. Membrane Sci. **126**, 151 (1997).
6. J. T. Yeh, L. H. Qang, K. N. Chen, and W. S. Jou, J. Mater. Sci. **36**, 1891 (2001).
7. C. Gagnard, Y. Germain, P. Keraudren, and B. Barriére, J. Appl. Polym. Sci. **92**, 676 (2004).
8. *Polymer Permeability*, Ed. by J. Comyn (Elsevier, New York, 1985).
9. R. M. Hodge, T. J. Bastow, G. H. Edward, G. P. Simon, and A. J. Hill, Macromolecules **29**, 8137 (1996).
10. T. J. Bastow, R. M. Hodge, and A. J. Hill, J. Membrane Sci. **131**, 207 (1997).
11. T. Terao, S. Maeda, and A. Saika, Macromolecules **16**, 1535 (1983).
12. S. Lai, M. Casu, G. Saba, A. Lai, I. Husu, G. Masci, V. Crescenzi, G. Masci, and V. Crescenzi, Solid State Nucl. Magn. Reson. **21**, 187 (2002).
13. M. Kobayashi, M. Kanekiyo, I. Ando, and S. Amiya, Polymer Gels and Networks **6**, 425 (1998).
14. M. Kobayashi, I. Ando, T. Ishii, and S. Amiya, Macromolecules **28**, 6677 (1995).
15. M. Kobayashi, I. Ando, T. Ishii, and S. Amiya, J. Mol. Struct. **440**, 155 (1998).
16. R. Ricciardi, C. Gaillet, G. Ducouret, F. Lafuma, and F. Lauprétre, Polymer **44**, 3375 (2003).
17. F. Horii, S. Hu, K. Deguchi, H. Sugisawa, H. Ohgi, and T. Sato, Macromolecules **29**, 3330 (1996).
18. K. Masuda and F. Horri, Macromolecules **31**, 5810 (1998).
19. K. Masuda, H. Kaji, and F. Horri, Polym. J. **31**, 105 (1999).
20. K. Masuda, H. Kaji, and F. Horri, J. Polym. Sci. Pol. Phys. **38**, 1 (2000).
21. K. Masuda, H. Kaji, and F. Horri, Polym. J. **33**, 190 (2001).
22. K. Masuda, H. Kaji, and F. Horri, Polym. J. **33**, 356 (2001).
23. H. Ohgi, H. Yang, T. Sato, and F. Horii, Polymer **48**, 3850 (2007).
24. N. Chen, L. Li, and Q. Wang, Plast. Rubber Compos. **36**, 284 (2007).

25. *Lange's Handbook of Chemistry*, Ed. by J. A. Dean, 15th ed. (McGraw-Hill, New York, 1999).
26. *Recommended Reference Materials for the Realization of Physicochemical Properties*, Ed. by K. N. Marsh (Blackwell Scientific, Oxford, 1987).
27. W. B. Li, F. Xue, and R. S. Cheng, Polymer **46**, 12026 (2005).
28. S. S. Wong, S. A. Altinkaya, and S. K. Mallapragada, Polymer **45**, 5151 (2004).
29. *Hansen Solubility Parameters: a User's Handbook*, Ed. by C. M. Hansen, 2nd ed. Taylor & Francis, New York, 2007).
30. *Plastic Packaging Materials for Food*, Eds. by O. G. Piringer and A. L. Baner (Wiley-Vch Verlag Gmbh, Malden, 2000).
31. V. J. McBrierty, F. X. Quinn, C. Keely, A. C. Wilson, and G. D. Friends, Macromolecules **25**, 4281 (1992).
32. D. Capitani, G. Mensitieri, F. Porro, N. Proietti, and A. L. Segre, Polymer **44**, 6589 (2003).
33. J. M. Lagaron, A. K. Powell, and G. Bonner, Polym. Test **20**, 569 (2001).
34. A. T. Dibenedetto, J. Polym. Sci. **A1**, 3459 (1963).
35. A. T. Dibenedetto, J. Polym. Sci. **A1**, 3477 (1963).
36. J. S. Vrentas and J. L. Duta, J. Polym. Sci. Pol. Phys. **15**, 403 (1977).
37. L. Fritz and D. Hofmann, Polymer **38**, 1035 (1997).
38. *Diffusion in Polymer*, Ed. by P. Neogi (Marcel Dekker, New York, 1996).
39. A. D. L. Rosa, L. Heux, and J. Y. Cavaillé, Polymer **41**, 7547 (2000).
40. Q. Yu, M. Zhou, Y. Ding, B. Jiang, and S. Zhu, Polymer **48**, 7058 (2007).
41. F. Horii, S. Hu, T. Ito, H. Odani, S. Matsuzawa, and K. Yamaura, Polymer **33**, 2299 (1992).